





## Highly stretchable electrochromic hydrogels for use in wearable electronic devices†

Guojian Yang, Jiale Ding, Baige Yang, Xiaojun Wang, Chang Gu, Dehui Guan, Yang Yu, Yu-Mo Zhang \* and Sean Xiao-An Zhang 

Cite this: *J. Mater. Chem. C*, 2019, **7**, 9481

Received 20th May 2019,  
Accepted 11th July 2019

DOI: 10.1039/c9tc02673h

rsc.li/materials-c

Even though several stretchable electrochromic (EC) materials have been reported, effective and facile strategies for the development of ideal intrinsically stretchable EC materials with various colors, simple preparation, low energy consumption, excellent performance, and practicability are still urgently required. Herein, an ideal inherently stretchable EC device is demonstrated and constructed by combining a novel intrinsically stretchable EC material as well as new asymmetric stretchable conductive electrodes where Ag nano-wires are used as the cathode and Au nanosheets are used as the anode in order to balance the conductivity, transmittance, stability, and mechanical properties. A stretchable EC material containing a highly transparent, elastic, and conductive polyacrylamide (PAAM) hydrogel and some new water-soluble EC molecules exhibits easily selectable multicolor-tunable property, desirable coloration efficiency with low energy consumption, and health- and environment-friendly characteristics. Further, color changes in the device can be easily and reversibly manipulated in seconds from yellow to red or brown under tensile strain. These promising results reveal that this new method/process is easily applicable and has promising potential for future wearable electronic displays.

### 1. Introduction

In recent years, wearable electronic displays have attracted considerable attention due to their comfortable features, such as portability and high flexibility.<sup>1–4</sup> Until now, various fascinating devices have been designed and demonstrated, such as OLEDs,<sup>5,6</sup> LEDs,<sup>7,8</sup> liquid crystal displays (LCDs),<sup>9</sup> and electrochromic devices (ECDs).<sup>10–15</sup> Among them, stable, and stretchable ECDs have been long anticipated and smartly constructed, which can retain their

structural integrity under strain and are very close to the requirements of an ideal wearable display. Such stretchable devices based on electrochromism exhibit more intriguing features, such as eye-friendly readability, less energy consumption, rich colors, and low cost.<sup>21–24</sup> A series of promising prototype devices have been accordingly fabricated with various electrochromic (EC) materials such as metal oxides,<sup>10</sup> organic molecules,<sup>12,15</sup> and polymers.<sup>11,13,14</sup> The realization of the desired stretchability usually necessitates complicated structural designs and expert skills to fabricate such special materials and deposit a rigid functional material onto a prestrained substrate or the surface with a microscale wavelike structure.<sup>1–3</sup> In order to simplify the fabrication process and improve the durability of the device for feasible future industrialization, many remarkable researchers have investigated “intrinsically stretchable EC” materials. For example, Nishizawa’s group cleverly developed a stretchable EC film that is a uniform composite of an inelastic EC polymer (poly(3,4-ethylenedioxythiophene)-*p*-toluene sulfonic acid) and elastic polymer (polyurethane).<sup>13</sup> Moreover, Odriozola’s group wisely developed a PVA–borax-based stretchable EC hydrogel that was appropriately combined with an EC molecule (ethyl viologen) for the first time.<sup>15</sup> Further, an ideal color diversity based on PVA–borax EC hydrogels was extended *via* several remarkable studies.<sup>16–20</sup> These earlier works have significantly accelerated the research and development (R&D) of the thriving field of wearable electronics. However, related progresses for practical industrialization seem to be dissatisfactory, particularly in the field of “intrinsically stretchable EC” materials. Several difficult obstacles still exist that significantly restrict the R&D of practicable stretchable ECDs such as follows: (a) there is still a long way to go to realize a high-performance full color desirable display; (b) the coloration efficiency is still not sufficiently high for desirable information display; (c) toxicity, environment, and health issues still exist during the preparation and utilization of related materials/devices; and (d) undesirable production costs and profits due to the complicated synthesis processes and difficulty to scale up.<sup>24</sup> Obviously, a novel “intrinsically stretchable EC” material with ideal characteristics is urgently needed,

State Key Lab of Supramolecular Structure and Materials, College of Chemistry, Jilin University, 130012 Changchun, P. R. China. E-mail: zhangyumo@jlu.edu.cn

† Electronic supplementary information (ESI) available: Experimental details, characterization of stretchable electrochromic hydrogels, characterization of stretchable electrodes, the performance of the stretchable electrochromic devices. See DOI: 10.1039/c9tc02673h

such as easily selectable multicolor-tunable property, desirable coloration efficiency with low energy consumption, health- and environment-friendly, low cost, easy scale-up ability, and having an ideally and universally applicable methodology.

Herein, a new prototype device with certain worthwhile characteristics of “intrinsically stretchable EC” materials has been formulated. This has been achieved by combining a highly transparent, elastic, and conductive polyacrylamide (PAAM) hydrogel electrolyte with some unusual water-soluble multi-colorable EC molecules based on the theory of “reversible electrobase.”<sup>25–28</sup> To achieve the ideal properties of fully stretchable and wearable electronics, particularly suitable for eye-friendly high-quality reflective information displays, we fabricated unconventional electrode sets, with the ability to transmit single light, by using Au nanosheets as the anode and Ag nanowires as the cathode. Here, Au nanosheets acted both as the counter electrode with very good conductivity and electrochemical stability as well as an eye-friendly pastel color background for reading information. Further, Ag nanowires in the top layer as the cathode could not only prevent oxidation, but also facilitate high-quality information display due to their good conductivity and high transparency. Based on the above materials, a promising prototype device was facilely and efficiently fabricated by embedding the new EC hydrogel into the electrode sets. Such a device could be distinctively changed from pale yellow to bright red or dark brown even under significant pulling or bending strain. Furthermore, it exhibited good reversibility without degradation observable even after 100 cycles under tension. The results indicate that such stretchable multicolor-tunable ECDs based on highly EC hydrogels should have promising potential for use in wearable displays.

## 2. Results and discussion

In order to fabricate intrinsically stretchable EC materials, a simple and facile method involved a combination of stretchable transparent electrolyte with the EC molecules. Therefore, a stretchable transparent electrolyte with high conductivity is an indispensable component. In this work, the PAAM hydrogel with KCl was selected as the ideal electrolyte. The preparation process is available in the ESI.† The prepared hydrogel electrolyte was referred to as hydrogel-1 and its tensile performance is shown in Fig. 1a. It could be stretched up to 7 times from its initial length, which meant that hydrogel-1 was an ideal material with good elasticity. The transmittance of hydrogel-1 was as high as 95% in the visible-light region, as shown in Fig. 1b. For the stretchable electrolyte, apart from high transmittance, the high strength and stability of ion conductivity during the stretching process were also important. In Fig. 1c and Fig. S1 (ESI†), it is evident that high ion conductivity (as high as  $1.07 \Omega \text{ m}$ ) was observed at the released state; the conductivity would marginally decrease when the strain was increased from 0% to 100%. From Fig. 1d, it is evident that the tensile performance was worthwhile, where the initial length could be achieved when the strain was released after 1000 stretching–releasing cycles with no observable

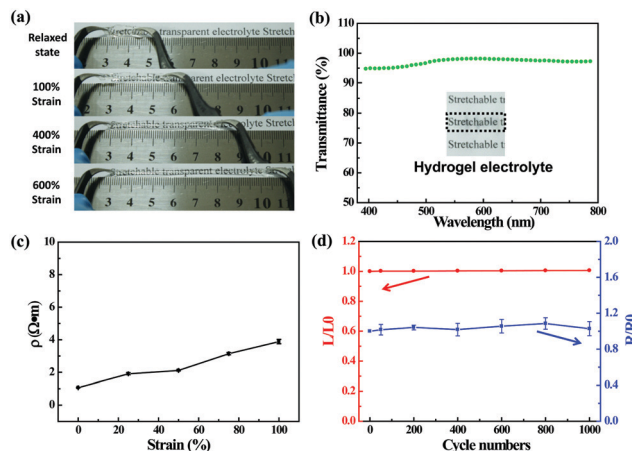


Fig. 1 Performance of hydrogel electrolyte (hydrogel-1). (a) Physical display of tensile performance. (b) Transmittance of hydrogel-1. (c) Electric resistivity at different strain values. (d) Changes in length and conductivity after 1000 cycles at 50% strain.

decrease in conductivity. Therefore, PAAM hydrogel with KCl exhibited the ideal performance as a stretchable transparent electrolyte.

It is well known that hydrogels can capture ambient water. That means the functional molecules dissolved in water could be inserted into a network of PAAM hydrogel by a one-step swelling process. Therefore, water-soluble materials with high EC performance should be developed. In this work, water-soluble EC materials based on the “reversible electrobase” theory were firstly reported, which could be combined with a hydrogel electrolyte. Fortunately, the traditional “electrobase” *p*-benzoquinone (*p*-BQ) exhibited good water solubility and it could efficiently work to regulate the color of the base-responsive water-soluble molecules. Here, thymol blue sodium salt (M-G) and phenol red sodium salt (M-R) with excellent water solubilities were chosen as the base-responsive molecules. Taking the combination of “*p*-BQ” and M-R as the example, the EC mechanism could be determined, as shown in Fig. 2a and b. In the network of PAAM hydrogel, *p*-BQ and M-R were uniformly distributed in the initial state. When a suitable bias voltage was applied, the neutral *p*-BQ would be reduced to the radical anion (*p*-BQ<sup>•−</sup>) with the generation of strong alkalinity. The proton of the surrounding M-R would be captured by the electrobase *p*-BQ<sup>•−</sup> and the color of the hydrogel changed from yellow to red. Moreover, the red state could return to the original yellow state when *p*-BQ<sup>•−</sup> was oxidized by the application of an opposite voltage. This implied that *p*-BQ could replace the chemical base to regulate the color of the base-responsive molecules in a closed water system.

In order to verify the feasibility of *p*-BQ as the “electrobase” to regulate the various base-responsive molecules, the reduction potentials of *p*-BQ and base-responsive molecules, respectively, and a mixture in deionized water and hydrogel matrix were measured, as shown in Fig. S2a–d (ESI†). The reduction peak of *p*-BQ was at  $-0.12 \text{ V}$ , while the reduction peaks of M-R and M-G were below  $-0.60 \text{ V}$ . The big gap in the reduction potentials ensured that the base-responsive molecules would not be

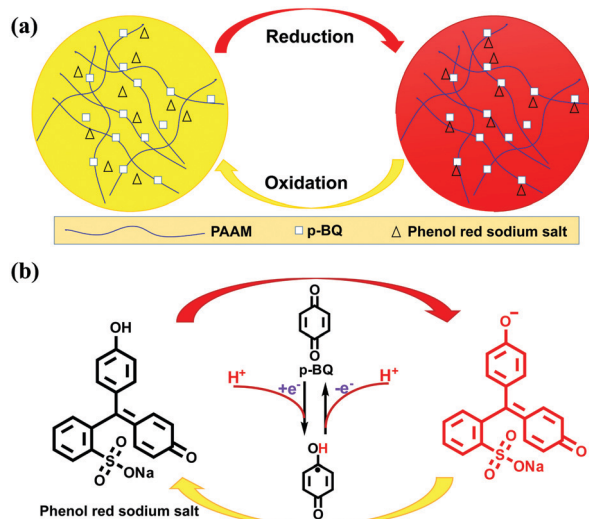


Fig. 2 Mechanism of water-soluble "electrobase" theory. (a) Schematic diagram of color switching when using *p*-BQ and M-R in hydrogel-1. (b) Color-switching mechanism induced by *p*-BQ as the "electrobase".

reduced under the reduction potential of *p*-BQ. Further, to investigate the optical changes during the CVs, the spectro-electrochemistry was measured "in situ" (Fig. S2e and f, ESI†) and the apparent changes in absorbance could be found only in the mixture of *p*-BQ and base-responsive molecule (M-R/M-G). In addition, the regulating process was totally reversible.

Furthermore, the UV-vis spectra of the mixture of *p*-BQ and M-R (or M-G) at  $-0.5$  V were investigated *in situ*, as shown in Fig. S3 (ESI†). The color of the solution containing *p*-BQ and M-G changed from yellow to blue as the absorption peak changed from 438 to 595 nm when the voltage was equivalent to the reduction potential of *p*-BQ. Further, the solution with M-R and *p*-BQ changed from yellow to purple as the absorption peak changed from 438 to 559 nm under the same test conditions. Moreover, the changes in color and absorption peaks were the same as those for M-G and M-R after adding the chemical base NaOH, as shown in Fig. S4 (ESI†). This implies that *p*-BQ could work as a base controlled by the electricity and *p*-BQ and M-G (*p*-BQ and M-R) system could serve as the water-soluble EC material. To further investigate the performance of water-soluble EC systems, liquid devices were fabricated, as shown in Fig. S5 and S6 (ESI†). Both these devices exhibited promising EC performances with fast open speed ( $<100$  ms) and ideal reversibility ( $>200$  cycles). Therefore, the EC system based on water-soluble molecules could be successfully fabricated.

Based on the above stretchable transparent electrolyte and water-soluble EC system, stretchable EC materials (EC hydrogel) could be easily developed, as shown in the ESI†. The device was fabricated by putting the EC hydrogel into a shaped polydimethylsiloxane (PDMS) spacer between two ITO glasses, as shown in Fig. 3a. It could be patterned with various shapes of PDMS spacers, and multicolor-tunable properties could be realized by changing the base-responsive molecules. The transmittance of such devices was very high such that the letters below the devices were clearly visible (Fig. 3b). The hydrogel-G device (M-G as the

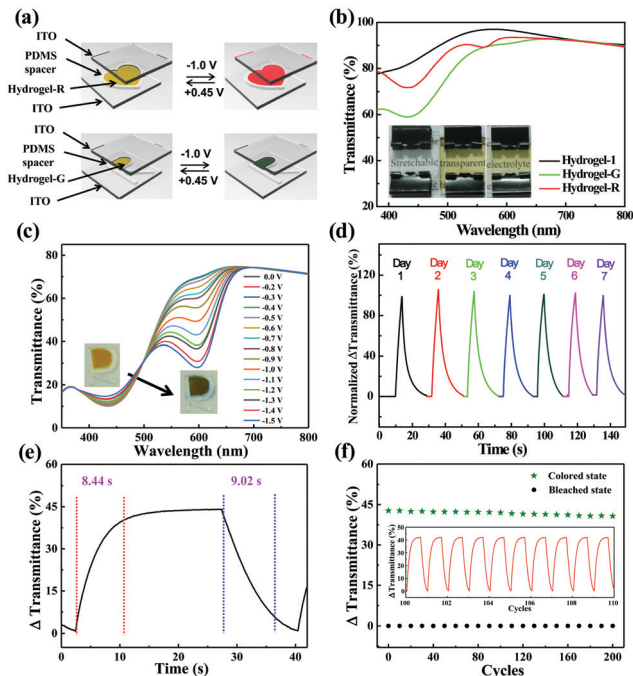


Fig. 3 (a) Device structure of ECDs containing EC hydrogel and the patterns by changing the shape of the PDMS spacer. (b) Transmittances of the devices containing hydrogel-1, hydrogel-G (M-G as the base-responsive molecule), and hydrogel-R (M-R as the base-responsive molecule). (c) Transmittance spectra of the hydrogel-G device under different voltages. (d) Stability of the switching behavior of the hydrogel-G device (normalized transmittance graph). (e) Response time of the hydrogel-G device during the coloring and bleaching processes. (f) Changes in the transmittance (595 nm) variation with switch cycles by alternative voltages of  $-1.1$  V (25 s) and  $+0.45$  V (13 s).

base-responsive molecule) could change its color from yellow to green under a voltage above  $-0.8$  V, as shown in Fig. 3c. Further, this process was reversible (Fig. S7, ESI†). One of the most important parameters for ECDs that can be employed in daily life is stability, which ensures that devices can be used for a longer time. From Fig. 3d, it is evident that the performance remained almost the same when the device switched colors for a week. Further, the response time was measured with respect to the coloring time (8.44 s) and bleaching time (9.02 s), as shown in Fig. 3e. The speed could ensure potential applications in smart windows and reflective displays. Moreover, the reversibility was ideal such that the intensity of color slightly decreased after 200 switching cycles between the maximum colored state and totally bleached state (Fig. 3f). It is well known that the equality between the absorbance (*A*) and transmittance (*T*) can be expressed as  $A = -\lg T$ , according to the Beer-Lambert law. Therefore, to reveal additional optical information of the device for applications involving different voltage programs, the corresponding absorption graphs of Fig. 3c–f are shown in Fig. S8 (ESI†).

The hydrogel-R device (M-R as the base-responsive molecule) also exhibited the ideal EC performance, as shown in Fig. S9 (ESI†). The coloration efficiency is an important parameter that can be used to measure the electron utilization efficiency of devices. The coloration efficiency of the hydrogel-R device was  $291.35 \text{ cm}^2 \text{ C}^{-1}$ , while that for the hydrogel-G device



was  $152.18 \text{ cm}^2 \text{ C}^{-1}$  (Fig. S10, ESI†). Moreover, traditional EC materials such as methyl viologen can also be combined with hydrogel-1. When the functional molecule was changed to methyl viologen, it exhibited good EC performance. As shown in Fig. S11 (ESI†), the device could be reversibly changed from colorless to purple, and it had a relatively low open voltage ( $-1.0 \text{ V}$ ) and good cycle stability. This implied that hydrogel-1 combined with a water-soluble EC system could be seen as a universal solution to fabricate intrinsically stretchable EC materials.

After the fabrication of highly stretchable EC hydrogels, it was necessary to apply them in stretchable ECDs with stretchable electrodes. Ag nanowires combined with PDMS are the most commonly used electrodes due to their high transmittance and high flexibility.<sup>29–31</sup> However, Ag nanowires could get easily oxidized at the anode in ECDs.<sup>12</sup> As shown in Fig. S12 (ESI†), the oxidation peak of Ag is  $+0.08 \text{ V}$ , whereas Au does not get oxidized below  $+0.4 \text{ V}$ . This implies that Au exhibits better electrochemical stability. Therefore, in this study, a novel asymmetrical electrode structure was designed and fabricated by combining the Au anode and Ag cathode to balance conductivity, transmittance, and stability. In earlier research works, transmissive and reflective ECDs have been developed for various applications. For example, transmissive ECDs can be used for smart windows and controlled reflectance mirrors,<sup>32,33</sup> while reflective devices are suitable for nonemissive displays such as e-paper, billboards, and so on.<sup>34,35</sup> When applied into the display area, the yellow background formed by the close-packing structure of Au nanosheets is suitable for reading, as shown in Fig. 4a. An electrode with Au nanosheets for ECDs was fabricated, as shown in Fig. S13 (ESI†). Au nanosheets were produced by a one-step hydrothermal synthesis process. To enhance the adhesion of Au nanosheets with the PDMS surface, a functional group ( $-\text{SH}$ ) was formed on the surface of the PDMS by the reaction of (3-mercaptopropyl)trimethoxysilane (MPTMS) with PDMS after hydrophilic treatment. The strong binding of  $-\text{SH}$  and Au was beneficial toward the enhancement of the interaction force of Au nanosheets and PDMS to improve the mechanical stability of the Au nanosheets as the electrode. The conductivity of the Au nanosheets as the electrode was about  $5 \Omega \text{ sq}^{-1}$ , which was superior to those of the conductive electrodes. Then, the tensile performance

of Au nanosheets as the electrode was measured. It could be stretched under strain, and it fully recovered when the strain was released (Fig. 4a). Further, the conductivity was stable when the electrode was subjected to 30% strain, as shown in Fig. 4b and c. However, the conductivity was marginally increased for strain exceeding 30%, which can be attributed to the changes in the morphology after the application of various strain values, as shown in Fig. S14 (ESI†). The combination of Au nanosheets was really tight when the strain was small. However, under large strain (such as 50%), the film of Au nanosheets broke with a fissure, which resulted in an irreversible decrease in conductivity. Moreover, the stability of conductivity was tested as stress was repeatedly added. When the electrode was stretched to 20% strain and recovered after 1000 cycles, the length of the electrode returned to its initial state and the sheet resistance marginally increased. This implied that the tolerance of the electrode was excellent. Therefore, Au nanosheets could function as an ideal material as ECD electrodes.

However, the top electrode should be highly transparent so that it does not influence information display. Therefore, stretchable Ag electrodes were fabricated by spin-coating on a DOPA-modified PDMS under a prestrained state, as shown in Fig. 5a. PDMS was initially modified with polydopamine to form a hydrophilic surface and the contact angle decreased from  $105.4^\circ$  to  $43.7^\circ$ , as shown in Fig. S15 (ESI†). The transmittance and conductivity of the electrode were dependent on the concentration of Ag nanowires, spin speed, and spin layers. Further, the spin-coating condition was optimized, as shown in Fig. S16 (ESI†). The best condition was Ag nanowire concentration of  $3 \text{ mg mL}^{-1}$ , spin speed of  $1000 \text{ rpm}$ , and solution of  $20 \mu\text{L}$  for  $10 \text{ s}$  for five times. Further, the best electrode performance was  $10 \Omega \text{ sq}^{-1}$  when the transmittance at  $550 \text{ nm}$  was  $80\%$ , as shown in Fig. 5b, which was similar than those of commercialized ITO and FTO electrodes. The morphology of the Ag nanowires as the electrode was confirmed by SEM, as shown in Fig. S17 (ESI†); evidently, Ag nanowires were uniformly distributed on the surface of PDMS as a network and they were interconnected, which improved the electrode performance. As a stretchable electrode, they could be easily twisted, stretched, and bent (Fig. 5c). Moreover, the change in sheet resistance of

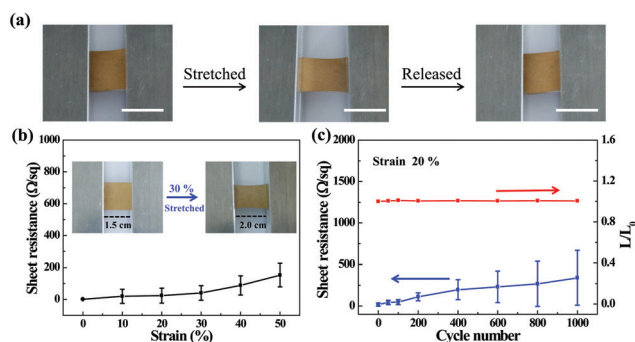


Fig. 4 (a) Display with Au nanosheets as the electrode after being stretched and released (scale bar:  $1 \text{ cm}$ ). (b) Sheet resistance of Au nanosheets as the electrode at different strain values. (c) Cycle performances of conductivity and length of Au nanosheets as the electrode when stretched to 20% strain for 1000 cycles.

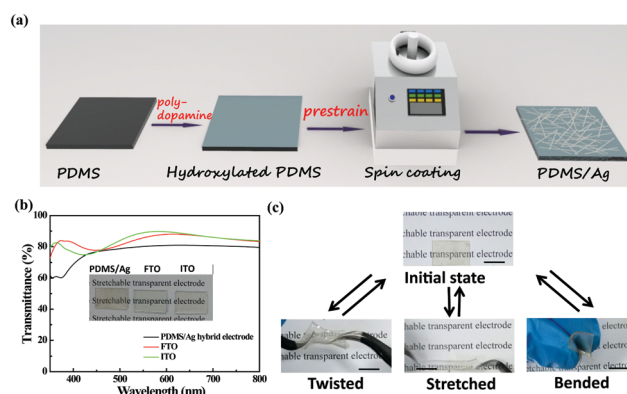


Fig. 5 (a) Schematic diagram of fabricating Ag nanowires as the electrode. (b) Transmittances of a commercial ITO electrode ( $R_s = 10 \Omega \text{ sq}^{-1}$ ), FTO electrode ( $R_s = 8 \Omega \text{ sq}^{-1}$ ), and Ag nanowires as the electrode ( $R_s = 10 \Omega \text{ sq}^{-1}$ ). (c) Tensile performance of the electrode (scale bar:  $1 \text{ cm}$ ).

the Ag nanowires as the electrode at different strain values and the durability of this electrode during cycle testing have been investigated, as shown in Fig. S18 (ESI†). Evidently, the conductivity decreased when the strain on the electrode was changed from 0% to 30%, which can be attributed to the increase in the electronic transmission distance. Further, the length of the electrode could completely return to its initial state after 600 cycles in cases where the electrode was stretched under 20% strain and then recovered. The conductivity exhibited a downward trend after several cycles, partly because the adhesive force of the Ag nanowires with the substrate (PDMS) was weaker than earlier.<sup>36,37</sup> From the above results, it can be concluded that the combination of PDMS and Ag nanowires could be used as a cathode for stretchable ECDs.

After the fabrication of intrinsically stretchable EC hydrogels and the development of a suitable electrode structure, stretchable devices comprising a combination of all the above stretchable parts could be fabricated. They can be worn on the wrist as a wearable smart electronic device, as shown in Fig. 6a. The EC hydrogel was put into such a PDMS spacer that all the parts of the ECD could become stretchable, which improved the tensile performance. Taking hydrogel-R as the example, it was evident that the device reversibly changed from yellow to red under voltages (Fig. 6b). The colors of these novel stretchable ECDs could be modulated by changing the type of hydrogel (Fig. S19, ESI†). In Fig. 6c, it is evident that the ECD based on hydrogel-R could be reversibly stretched and the color of the device could be reversibly changed from yellow to red. This implied that the device exhibited worthwhile EC performances at both relaxed and stretched states. As evident from the cross section when the device was bent (Fig. 6d), all the parts of the device were tightly connected when the shape of the device underwent a significant change. Moreover, the device could be twisted and reversibly recovered, as shown in Fig. S20 (ESI†). This

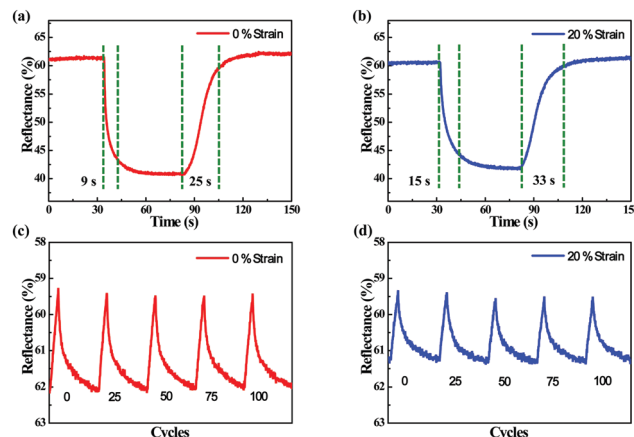


Fig. 7 Switching behavior of the device (559 nm) at 0% strain (a) and 20% strain (b). Cycle stability of the device (559 nm) at 0% strain (c) and 20% strain (d).

impressive phenomenon facilitated the maintenance of the EC performance when the device was stretched.

For our stretchable ECD, the coloration efficiency was  $92.10 \text{ cm}^2 \text{ C}^{-1}$  (Fig. S21, ESI†), which was higher than those reported for stretchable ECDs, as listed in Table S1 (ESI†). To determine the change in the EC performance for the device under strain, the response time and cycle stability were tested for different strain values. In Fig. 7a and b, it is evident that the coloring time of the device increased from 9 to 15 s and the bleaching time increased from 25 to 33 s when the device was stretched to 20% strain under the same stimulating voltages. This might be because the resistance of the device marginally increased when the device was stretched. However, it still relatively maintained its high coloring properties, although the response time increased. Moreover, the cycle stabilities of the device at 0% and 20% strain were measured, as shown in Fig. 7c and d. Evidently, the device could maintain its performance after about 100 cycles even at 20% strain. Further, we compared the EC performances of these stretchable devices with the other stretchable devices reported in recent years, as shown in Table S1 (ESI†). Different materials such as metal oxides ( $\text{WO}_3$ ), organic molecules (ethyl viologen and  $\text{HV}(\text{BF}_4)_2$ ), and EC polymers (P3HT and PEDOT/PU) have been used to fabricate devices with single-color switching, whereas the device formulated in this study has an ideal multicolor-tunable property. Moreover, the device reported in our work has relatively high coloration efficiency as compared to the other devices. This device was totally environmentally friendly and nontoxic because the preparation process did not involve the usage of organic solvents as well as the fact that PAAM hydrogel is nonharmful to humans. Further, our work yielded an ideal response speed and relatively improved reversibility. Therefore, the stretchable ECDs formulated in this study have the potential to be applied in social life.

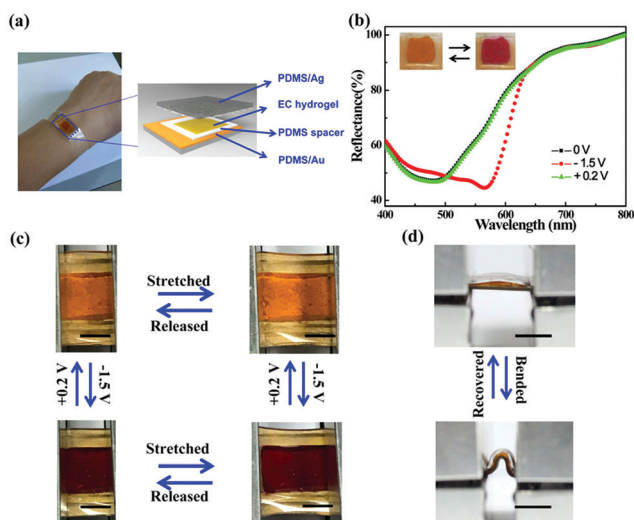


Fig. 6 (a) Schematic diagram of the structure of stretchable ECD which worn on the wrist. (b) Reflectance values of the hydrogel-R device at different voltages. (c) Physical display of the ECD with deformable performance from top section (scale bar: 1 cm). (d) Physical display of ECD when bent from the cross section (scale bar: 1 cm).

### 3. Conclusions

In conclusion, a new method for fabricating an intrinsically stretchable ECD has been reported by combining an intrinsically

stretchable EC hydrogel and new asymmetric stretchable electrodes containing Au nanosheets as the anode and Ag nanowires as the cathode. It exhibited promising performance with high coloration efficiency ( $291.35 \text{ cm}^2 \text{ C}^{-1}$  for hydrogel-R and  $152.18 \text{ cm}^2 \text{ C}^{-1}$  for hydrogel-G), good reversibility ( $>200$  cycles), and short open time ( $<100$  ms) when applied into ECDs using ITO glass as the electrode. Further, a stretchable multicolor-tunable ECD was integrated by combining the intrinsically stretchable EC hydrogel and a new asymmetric electrode structure containing Au nanosheets as the anode and Ag nanowires as the cathode. The color change of the device could be easily and reversibly manipulated from yellow to red or brown under tensile strain. These promising results reveal that this new method/process is easily applicable and has promising potential for use in future wearable electronic displays.

## Conflicts of interest

There are no conflicts to declare.

## Acknowledgements

We thank the National Natural Science Foundation of China (No. 21602075, 21875087) and Natural Science Foundation of Jilin Province (CN) (No. 20180520155JH) for financial support.

## Notes and references

- J. A. Rogers, T. Someya and Y. Huang, *Science*, 2010, **327**, 1603–1607.
- S. Wagner and S. Bauer, *MRS Bull.*, 2012, **37**, 207–213.
- D. H. Kim and J. A. Rogers, *Adv. Mater.*, 2008, **20**, 4887–4892.
- M. Gao, L. Li and Y. Song, *J. Mater. Chem. C*, 2017, **5**, 2971–2993.
- D. Yin, J. Feng, R. Ma, Y.-F. Liu, Y.-L. Zhang, X.-L. Zhang, Y.-G. Bi, Q.-D. Chen and H.-B. Sun, *Nat. Commun.*, 2016, **7**, 11573–11579.
- T. Sekitani, H. Nakajima, H. Maeda, T. Fukushima, T. Aida, K. Hata and T. Someya, *Nat. Mater.*, 2009, **8**, 494–499.
- S.-I. Park, Y. Xiong, R.-H. Kim, P. Elvikis, M. Meitl, D.-H. Kim, J. Wu, J. Yoon, C.-J. Yu, Z. Liu, Y. Huang, K.-C. Hwang, P. Ferreira, X. Li, K. Choquette and J. A. Rogers, *Science*, 2009, **325**, 977–982.
- M. Vosgueritchian, J. B.-H. Tok and Z. Bao, *Nat. Photonics*, 2013, **7**, 769–771.
- F. Castles, S. M. Morris, J. M. C. Hung, M. M. Qasim, A. D. Wright, S. Nosheen, S. S. Choi, B. I. Outram, S. J. Elston, C. Burgess, L. Hill, T. D. Wilkinson and H. J. Coles, *Nat. Mater.*, 2014, **13**, 817–821.
- C. Yan, W. Kang, J. Wang, M. Cui, X. Wang, C. Y. Foo, K. J. Chee and P. S. Lee, *ACS Nano*, 2014, **8**, 316–322.
- H.-H. Chou, A. Nguyen, A. Chortos, J. W. To, C. Lu, J. Mei, T. Kurosawa, W.-G. Bae, J. B.-H. Tok and Z. Bao, *Nat. Commun.*, 2015, **6**, 8011–8020.
- H.-S. Liu, B.-C. Pan and G.-S. Liou, *Nanoscale*, 2017, **9**, 2633–2639.
- H. Kai, W. Suda, Y. Ogawa, K. Nagamine and M. Nishizawa, *ACS Appl. Mater. Interfaces*, 2017, **9**, 19513–19518.
- H. Park, D. S. Kim, S. Y. Hong, C. Kim, J. Y. Yun, S. Y. Oh, S. W. Jin, Y. R. Jeong, G. T. Kim and J. S. Ha, *Nanoscale*, 2017, **9**, 7631–7640.
- Y. Alesanco, J. Palenzuela, A. Viñuales, G. Cabañero, H. J. Grande and I. Odriozola, *ChemElectroChem*, 2015, **2**, 218–223.
- C. Lee, Y. Oh, I. S. Yoon, S. H. Kim, B.-K. Ju and J.-M. Hong, *Sci. Rep.*, 2018, **8**, 2763.
- Y. Alesanco, A. Viñuales, J. Palenzuela, I. Odriozola, G. Cabañero, J. Rodriguez and R. Tena-Zaera, *ACS Appl. Mater. Interfaces*, 2016, **8**, 14795–14801.
- Y. Alesanco, A. Viñuales, G. Cabañero, J. Rodriguez and R. Tena-Zaera, *Adv. Opt. Mater.*, 2017, **5**, 1600989.
- Y. Alesanco, A. Viñuales, J. Ugalde, E. Azaceta, G. Cabañero, J. Rodriguez and R. Tena-Zaera, *Sol. Energy Mater. Sol. Cells*, 2018, **177**, 110–119.
- Y. Alesanco, A. Viñuales, G. Cabañero, J. Rodriguez and R. Tena-Zaera, *ACS Appl. Mater. Interfaces*, 2016, **8**, 29619–29627.
- M. Grätzel, *Nature*, 2001, **409**, 575–576.
- P. Andersson, R. Forchheimer, P. Tehrani and M. Berggren, *Adv. Funct. Mater.*, 2007, **17**, 3074–3082.
- G. Sonmez, C. K. F. Shen, Y. Rubin and F. Wudl, *Angew. Chem., Int. Ed.*, 2004, **116**, 1524–1528.
- G. Cai, J. Wang and P. S. Lee, *Acc. Chem. Res.*, 2016, **49**, 1469–1476.
- Y.-M. Zhang, M. Li, W. Li, Z. Huang, S. Zhu, B. Yang, X.-C. Wang and S. X.-A. Zhang, *J. Mater. Chem. C*, 2013, **1**, 5309–5314.
- Y.-M. Zhang, W. Li, X. Wang, B. Yang, M. Li and S. X.-A. Zhang, *Chem. Commun.*, 2014, **50**, 1420–1422.
- X. Wang, W. Li, W. Li, C. Gu, H. Zheng, Y. Wang, Y.-M. Zhang, M. Li and S. X.-A. Zhang, *Chem. Commun.*, 2017, **53**, 11209–11212.
- G. Yang, D. Guan, N. Wang, W. Zhang, C. Gu, Y.-M. Zhang, M. Li and S. X.-A. Zhang, *J. Mater. Chem. C*, 2017, **5**, 11059–11066.
- F. Xu and Y. Zhu, *Adv. Mater.*, 2012, **24**, 5117–5122.
- D. Langley, G. Giusti, C. Mayousse, C. Celle, D. Bellet and J.-P. Simonato, *Nanotechnology*, 2013, **24**, 452001.
- S. Ye, A. R. Rathmell, Z. Chen, I. E. Stewart and B. J. Wiley, *Adv. Mater.*, 2014, **26**, 6670–6687.
- R. Baetens, B. P. Jelle and A. Gustavsen, *Sol. Energy Mater. Sol. Cells*, 2010, **94**, 87–105.
- G. A. Niklasson and C. G. Granqvist, *J. Mater. Chem.*, 2007, **17**, 127–156.
- S. I. Cho, W. J. Kwon, S.-J. Choi, P. Kim, S.-A. Park, J. Kim, S. J. Son, R. Xiao, S.-H. Kim and S. B. Lee, *Adv. Mater.*, 2005, **17**, 171–175.
- X. W. Sun and J. X. Wang, *Nano Lett.*, 2008, **8**, 1884–1889.
- P. Lee, J. Lee, H. Lee, J. Yeo, S. Hong, K. H. Nam, D. Lee, S. S. Lee and S. H. Ko, *Adv. Mater.*, 2012, **24**, 3326–3332.
- D. Langley, G. Giusti, C. Mayousse, C. Celle, D. Bellet and J.-P. Simonato, *Nanotechnology*, 2013, **24**, 452001.